EARTHQUAKE ENGINEERING AND STRUCTURAL DYNAMICS, VOL. 25, 599–610 (1996)

CHARACTERISTICS OF TORSIONAL GROUND MOTIONS

H. HAO*

School of Civil and Structural Engineering, Nanyang Technological University, Nanyang Ave., Singapore 2263

SUMMARY

Due to the inherent difficulty in directly recording the rotational ground motions, torsional ground motions have to be estimated from the recorded spatially varying translational motions. In this paper, an empirical coherency function, which is based on the recorded motions at the SMART-1 array, is suggested to model the spatial variation of translational motions. Then, the torsional ground motion power spectral density function is derived. It depends on the translational motion power spectral density function and the coherency function. Both the empirical coherency function and the torsional motion power spectral density function are verified by the recorded motions at the SMART-1 array. The response spectra of the torsional motions are also estimated. Discussion on the relations between the torsional motion response spectrum and the corresponding translational motion response spectrum is made. Numerical results presented can be used to estimate the torsional ground motion power spectral density function and response spectrum.

KEY WORDS: torsional motion; coherency; phase shift; spectrum

INTRODUCTION

Properly defining torsional ground motion at a point on ground surface is critical in analysing the torsional responses of structures produced by torsional motions. Torsional ground motions are, however, difficult to be measured directly. In practice, only translational ground motions, either accelerations or displacements, are directly measured.[1] Torsional ground motions, as they are important to structural response analysis, are usually estimated from the spatially varying translational motions. Some methods were proposed to estimate the torsional motion,[2,3] but those methods considered only the phase shift of the propagating plane wave; the coherency loss effect due to wave propagation was not included. Torsional ground motions were also numerically estimated by using the recorded spatially varying translational motions during five earthquakes at the SMART-1 array.[4] In that study, however, only numerical values of the peak and central frequencies of the torsional motions were given. No explicit formula for estimating the torsional motions was presented. The relations between torsional motion and translational motion characteristics such as the power spectral density function and coherency function were not defined. Recently, numerical values of torsional ground motions were estimated again by using the recorded spatial translational motions at the basements of building structures during recent major earthquakes, and the estimated torsional accelerations were used to analyse the torsional responses of the building structures.[5]

In this study, the Power Spectral Density (PSD) function of torsional ground motion at a point on ground surface is derived as a function of the PSD and the coherency function of the horizontal spatially varying translational motions. As will be discussed, the previously proposed coherency functions,[6–9] which can model the torsional ground motion spatial variations well and were successfully applied to analyse the structural responses to spatially varying multiple excitations, cannot be used to model the torsional ground motions. A new form of empirical coherency function is thus suggested, which is obtained by processing the recorded motions at the SMART-1 array. The suggested coherency function in this study can be used to

* Senior Lecturer

CCC 0098–8847/96/060599–12

Received 7 March 1995
Revised 14 December 1995

model the torsional motion PSD. Numerical values of the torsional motion PSDs and the coherency functions of the motions recorded during Events 24 and 45 at the SMART-1 array are calculated to verify the proposed torsional motion PSD and the coherency function. Random vibration method is then employed to calculate the translational and torsional motion response spectra. The response spectrum ratios of the torsional to translational motions with respect to various ground motion spatial correlations and site conditions are calculated and presented. The effects of the coherency functions and the site conditions on the torsional motion response spectrum are discussed.

The primary objective of the present investigation is to study the characteristics of torsional ground motions and their relations to the corresponding translational motions in terms of their respective PSDs and response spectra.

COHERENCY FUNCTION

Using the recorded motions at the SMART-1 array, several empirical coherency functions were suggested.[6-9] The first three[6-8] are functions of the separation distance only, that is the spatial variation of ground motion is independent of the direction of ground motion propagation. The further study on the recorded motions,[9] however, revealed that ground motion spatial variation depends on the direction of wave propagation. The motions at the locations separated in the ground motion propagation direction tend to correlate less than those separated by the same distance but in its transverse direction. A two-dimensional coherency function was proposed,[9] which is a function of the frequency, apparent propagation velocity, and the square roots of the separation distances in the ground motion propagation direction and its transverse direction. As will be discussed in the next section, even though coherency functions[6-9] model the spatial variations of translational motions well, they cannot be used to model the torsional ground motions.

A new form of two-dimensional coherency function for ground motions at points k and l on ground surface is proposed as

$$\gamma_{kl}(x, y, \mathrm{i}\bar{\omega}) = |\gamma_{kl}| \exp\left(-\frac{\mathrm{i}\bar{\omega}x}{v_a}\right) = \exp[-(\alpha_1(\bar{\omega})x^2 + \alpha_2(\bar{\omega})y^2)\bar{\omega}] \exp\left(-\frac{\mathrm{i}\bar{\omega}x}{v_a}\right) \tag{1}$$

where $|\gamma_{kl}|$ is the coherency loss function and $\exp(-\mathrm{i}\bar{\omega}x/v_a)$ is the phase shift between the motions at the points k and l, and $\bar{\omega}$ is the circular frequency, v_a is the apparent ground motion propagation velocity, x and y are the separation distances between the points k and l in the ground motion propagation direction and its transverse direction, respectively; $\mathrm{i} = \sqrt{-1}$ is the imaginary unit; and $\alpha_1(\bar{\omega})$ and $\alpha_2(\bar{\omega})$ are the parameter functions with the form

$$\alpha_j(\bar{\omega}) = \frac{a_j}{\ln(\bar{\omega}) + b_j}, \quad \bar{\omega} \geqslant 0{\cdot}314 \text{ rad/s}, \; j = 1, 2 \tag{2}$$

in which a_j and b_j are determined by regressive method from the recorded motions, and $b_j > |\ln(0{\cdot}314)| = 1{\cdot}1584$.

The signal processing method is used to calculate the coherency functions of the recorded motions, which is defined as

$$\gamma_{kl}(x, y, \mathrm{i}\bar{\omega}) = \frac{S_{kl}(\mathrm{i}\bar{\omega})}{\sqrt{S_{kk}(\bar{\omega})\, S_{ll}(\bar{\omega})}} \tag{3}$$

where $S_{kk}(\bar{\omega})$ and $S_{ll}(\bar{\omega})$ are the PSDs of the motions at the points k and l, respectively; and $S_{kl}(\mathrm{i}\bar{\omega})$ is the cross PSD between the motions at the two points. The PSDs can be estimated by

$$S_{kl}(\mathrm{i}\bar{\omega}) = \frac{1}{T} \sum_{n=-M}^{M} W_n \bar{u}_k(\bar{\omega} + 2\pi n/T)\, \bar{u}_l^*(\bar{\omega} + 2\pi n/T) \tag{4}$$

where $\bar{u}_k(\bar{\omega})$ and $\bar{u}_l(\bar{\omega})$ are the Fourier transform of ground motion time histories at the points k and l, respectively; T is the duration of the motion; W_n is a smoothing window, $2M + 1$ is the number of points of the smoothing window, and $2\pi n/T = n\Delta\bar{\omega}$, in which $\Delta\bar{\omega}$ is the frequency increment, and the asterisk indicates the complex conjugate.

$S_{kk}(\bar{\omega})$ and $S_{ll}(\bar{\omega})$ are usually assumed to be the same in engineering application since the distance between any two points in an engineering site is relatively small compared to the epicentral distance. Thus, the change of the magnitude and frequency content in ground motion PSD due to motion propagating through an engineering site can be neglected.

The cross-correlation coefficient function between the recorded motions is

$$\rho_{kl}(\tau) = \frac{B_{kl}(\tau)}{B_{kk}(0)\, B_{ll}(0)} \tag{5}$$

where B_{kk}, B_{ll} and B_{kl} are the auto and cross-covariance functions of the motions recorded at the points k and l, and τ is the time lag. They can be estimated by

$$B_{kl}(m) = \begin{cases} \dfrac{1}{N}\displaystyle\sum_{n=1}^{N-m} u_k(n)\, u_l(n+m), & 0 \leqslant m \leqslant N \\ \dfrac{1}{N}\displaystyle\sum_{n=-m}^{N} u_k(n) u_l(n+m), & -N \leqslant m \leqslant 0 \\ 0, & |m| > N \end{cases} \tag{6}$$

where $N = T/\mathrm{d}t$ is the number of points of the ground motion time history, in which $\mathrm{d}t$ is the time increment; and the time lag $\tau = m\,\mathrm{d}t$. The ground motion apparent propagation velocity is estimated by determining its propagation time from the points k to l, which is the time lag corresponding to the highest absolute cross-correlation coefficient.

Using the recorded motions during Events 24 and 45 at the inner ring stations and the centre station, the coherency loss function between each pair of stations is calculated. Then the regression method is applied to determine the numerical values of a_j and b_j. The apparent velocity v_a is obtained by calculating the cross-correlation coefficient functions between motions at any two stations. The detailed information on the SMART-1 array and the procedure in data processing techniques can be found in references.[1,6–9] The numerical values of a_j, b_j and v_a for the two events are given in Table I.

Figure 1 shows the comparisons between the typical coherency loss values obtained from the proposed coherency function and those from the recorded motions calculated by equation (3). As can be seen, a very good agreement is achieved.

It should be noted that the coherency loss function and the apparent velocity are usually different if different time windows of a strong motion record are considered. In other words, strong ground motions are usually non-stationary. For example, it was found that the coherency losses and apparent velocities of P-, S- and surface waves vary considerably,[6,9] but there is no any general conclusion about the variations of the coherency loss and the apparent velocity in different time windows. Since ground motions are usually

Table I. Constants in coherency function

Event	a_1	b_1	a_2	b_2	v_a (m/s)
24	$1{\cdot}68934 \times 10^{-6}$	1·42983	$1{\cdot}74054 \times 10^{-6}$	1·57179	770
45	$1{\cdot}1167 \times 10^{-6}$	1·66726	$1{\cdot}1593 \times 10^{-6}$	1·72263	875

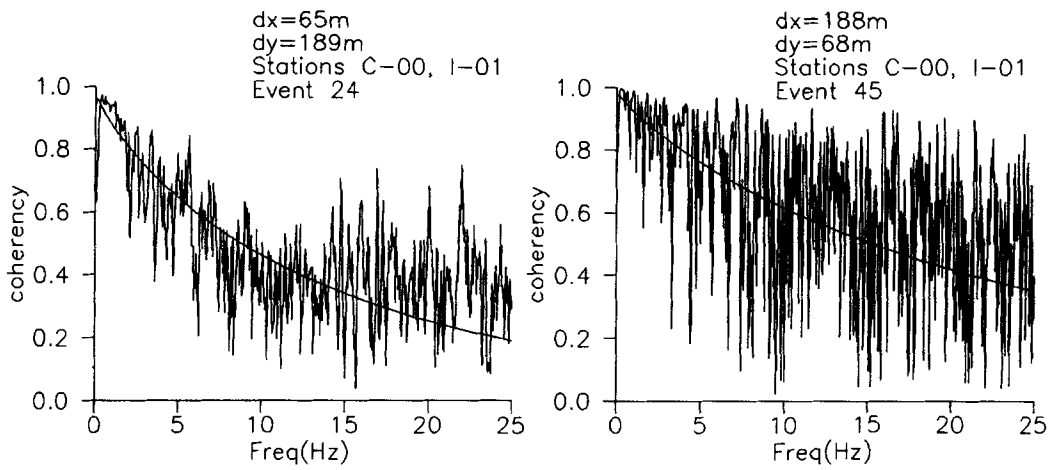

Figure 1. Model coherency loss functions and the estimated coherency loss between recorded spatial motions at the SMART-1 array

assumed to be stationary in engineering application, stationary assumption was also used to derive the coherency functions in the previous studies,[6-9] and the results obtained were proved yielding reliable estimation of the coherency loss and apparent velocity of spatially varying translational ground motions. For these reasons, stationary assumption is also adopted in this study so that the coherency loss and apparent velocity are assumed independent of the time windows.

TORSIONAL MOTION POWER SPECTRAL DENSITY FUNCTION

Let $\ddot{u}(x, y, t)$ and $\ddot{v}(x, y, t)$ be horizontal translational accelerations in the X and Y directions, respectively, the torsional acceleration can be defined according to the elastic mechanics as

$$\ddot{\phi}(t) = \tfrac{1}{2}\left[\frac{\partial \ddot{u}(x, y, t)}{\partial y} - \frac{\partial \ddot{v}(x, y, t)}{\partial x}\right]$$

$$= \tfrac{1}{2}\lim_{\substack{x\to 0\\ y\to 0}}\left[\frac{\ddot{u}(0, y, t) - \ddot{u}(0, 0, t)}{y} - \frac{\ddot{v}(x, y, t) - \ddot{v}(0, y, t)}{x}\right] \tag{7}$$

Assuming ground motion propagates in the X direction, then X direction is the ground motion principal direction and motions in the X and Y directions can be considered statistically independent.[1,10] By denoting $\ddot{u}(0, y, t)$, $\ddot{u}(0, 0, t)$, $\ddot{v}(x, y, t)$ and $\ddot{v}(0, y, t)$ by $\ddot{u}_2$, $\ddot{u}_1$, $\ddot{v}_2$ and $\ddot{v}_1$, respectively, the covariance function of $\ddot{\phi}(t)$ is

$$E[\ddot{\phi}(t+\tau)\ddot{\phi}(t)] = \tfrac{1}{2}\lim_{\substack{x\to 0\\ y\to 0}}\left\{\frac{E[\ddot{u}_2\ddot{u}_2] + E[\ddot{u}_1\ddot{u}_1] - E[\ddot{u}_1\ddot{u}_2] - E[\ddot{u}_2\ddot{u}_1]}{y^2}\right.$$

$$\left. + \frac{E[\ddot{v}_2\ddot{v}_2] + E[\ddot{v}_1\ddot{v}_1] - E[\ddot{v}_1\ddot{v}_2] - E[\ddot{v}_2\ddot{v}_1]}{x^2}\right\} \tag{8}$$

The PSD of the torsional acceleration is then obtained by transferring equation (8) into the frequency domain

$$S_{\ddot{\phi}}(\bar{\omega}) = \lim_{\substack{x\to 0\\ y\to 0}} \frac{1}{2}\left\{\frac{2S_g(\bar{\omega}) - 2S_g(\bar{\omega})\,\mathrm{Re}[\gamma_{kl}(0, y, \bar{\omega})]}{y^2} + \frac{2S_g(\bar{\omega}) - 2S_g(\bar{\omega})\,\mathrm{Re}[\gamma_{kl}(x, 0, \bar{\omega})]}{x^2}\right\}$$

$$= \lim_{\substack{x\to 0\\ y\to 0}} \left[\frac{1 - \exp[-\alpha_2(\bar{\omega})y^2\bar{\omega}]}{y^2} + \frac{1 - \exp[-\alpha_1(\bar{\omega})x^2\bar{\omega}]\cos(\bar{\omega}x/v_a)}{x^2}\right] S_g(\bar{\omega})$$

$$= S_g(\bar{\omega})\bar{\omega}[\alpha_1(\bar{\omega}) + \alpha_2(\bar{\omega}) + \bar{\omega}/2v_a^2] \tag{9}$$

where $S_g(\bar{\omega})$ is the PSD of the translational accelerations, which is assumed the same for motions in the X and Y directions and at every point in the site under consideration.

As can be noted in deriving equation (9), the exponential coherency loss function should be a function of the square of the separation distance, otherwise the torsional acceleration PSD will approach either zero or infinite as x and y approach zero depending on whether the power of the separation distance is greater or less than two. For that reason, the previously suggested coherency functions, which are either the exponential functions of the separation distance[6-8] or an exponential function of the square root of the separation distance,[9] could not be used to estimate the torsional acceleration PSD since they lead to infinite estimation.

The $\alpha_j(\bar{\omega})$'s are the parameter functions that determine the shape of the coherency loss function, while $\bar{\omega}/2v_a^2$ is related to the phase shift. Thus, the torsional motion PSD given in equation (9) depends on both the coherency loss and the phase shift of the spatially varying translational ground motions. From equation (9), it can also be noted that the torsional motion PSD has a higher-frequency content but lower amplitude than the corresponding translational motion PSD.

To verify the validity of equation (9), the torsional ground accelerations are estimated by using the recorded horizontal accelerations at every inner ring station and the centre station of the SMART-1 array during Events 24 and 45 by

$$\ddot{\phi}(t) = \frac{1}{2}\left[\frac{\ddot{u}_2(t) - \ddot{u}_1(t)}{y} - \frac{\ddot{v}_2(t) - \ddot{v}_1(t)}{x}\right] \tag{10}$$

where $\ddot{u}_j(t)$ and $\ddot{v}_j(t)$ are the recorded accelerations at the inner ring and the centre stations in the NS and EW directions, respectively. Figure 2 shows the typical recorded horizontal translational accelerations and the estimated torsional acceleration.

The PSD of each estimated torsional acceleration is calculated. Those of the same event are averaged to obtain the assemble average of the torsional acceleration PSDs for the two events.

Torsional acceleration PSDs of the two events are then estimated by using equation (9), where $S_g(\bar{\omega})$ is obtained by averaging the recorded translational acceleration PSDs at the inner ring and the centre stations of the two events separately. The parameters in functions $\alpha_j(\bar{\omega})$ and the apparent velocity given in Table I are used in the estimation. Figure 3 shows the comparisons between the torsional acceleration PSDs of the two events obtained by the two approaches. It can be seen that the magnitudes of the torsional motion PSDs of the two events estimated by equation (9) are slightly smaller at low frequencies and slightly larger at high frequencies than those estimated by using the recorded motions. Also, the torsional motion PSD of Event 45 shows a peak at 0·73 Hz, while the corresponding PSD from equation (9) does not have this peak. These discrepancies might be attributed to the errors induced by using the separation distances x and y to approximate their respective limits in equation (10), and to the use of the smoothed coherency functions. As can be seen in Figure 1, the actual coherency loss functions oscillate chaotically, while the coherency functions used for the torsional motion spectrum estimation are the best-fitted smooth functions. Nevertheless, the torsional PSDs estimated by equation (9) in general agree well with those obtained by direct calculation of the recorded spatially varying translational accelerations.

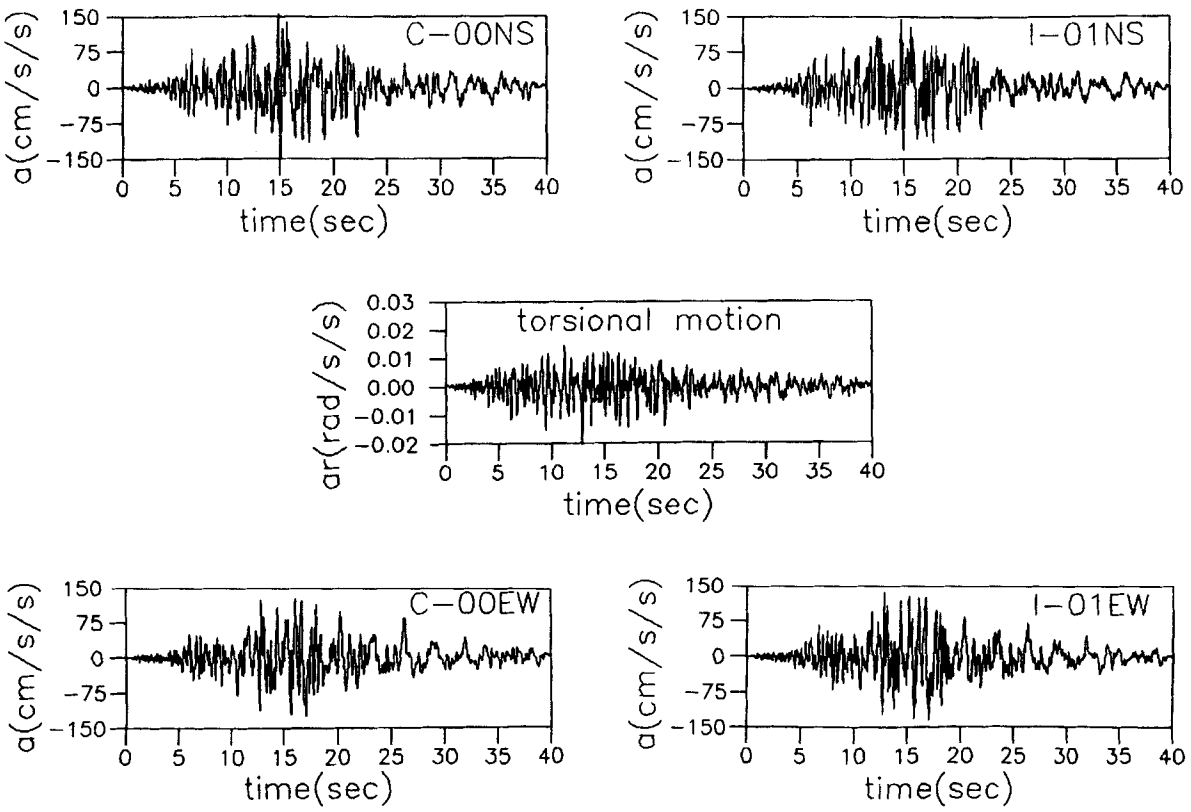

Figure 2. Recorded ground accelerations at stations C-00 and 1-01 of the SMART-1 array and the estimated torsional ground acceleration

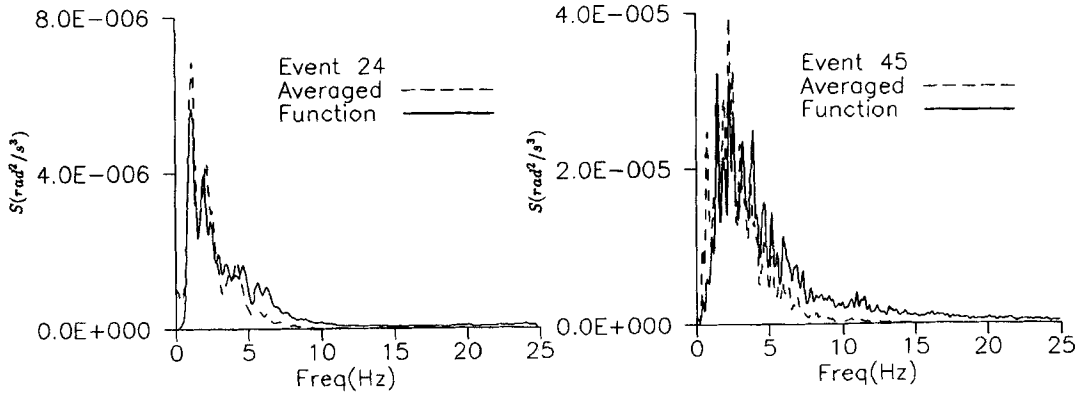

Figure 3. Comparison of the torsional motion power spectral density functions

TORSIONAL MOTION RESPONSE SPECTRUM

Torsional motion PSD estimated by equation (9) can be used to simulate torsional ground acceleration or directly used in spectrum analysis of the structural responses. In engineering practice, however, the response spectrum is the most commonly used quantity in analysis and design. The response spectrum can be estimated from the PSD by using the random vibration method.

Assuming earthquake ground motions are zero mean stationary Gaussian random processes, the PSD of the translational motion is usually modelled by a filtered Tajimi–Kanai spectrum[11] as given by

$$S_g(\bar{\omega}) = \frac{\bar{\omega}^4}{(\omega_1^2 - \bar{\omega}^2)^2 + 4\xi_1^2\omega_1^2\bar{\omega}^2} \frac{1 + 4\xi_g^2(\bar{\omega}^2/\omega_g^2)}{(1 - \bar{\omega}^2/\omega_g^2)^2 + 4\xi_g^2(\bar{\omega}^2/\omega_g^2)} \Gamma \tag{11}$$

where $\omega_1 = 1{\cdot}636$ rad/s, and $\xi_1 = 0{\cdot}616$ are the central frequency and damping ratio of the high-pass filter, ω_g and ξ_g are the central frequency and damping ratio of the Tajimi–Kanai PSD and they depend on the site conditions; and Γ is a scale factor depending on the ground motion intensity.

The displacement response PSD of a single-degree-of-freedom structure subjected to ground excitation with PSD $S_{\ddot{v}_g}(\bar{\omega})$ can be derived as

$$S_y(\bar{\omega}) = S_{\ddot{v}_g}(\bar{\omega})|H(\bar{\omega})|^2 \tag{12}$$

where

$$|H(\bar{\omega})|^2 = \frac{1}{(\omega_0^2 - \bar{\omega}^2)^2 + 4\xi^2\omega_0^2\bar{\omega}^2} \tag{13}$$

is the transfer function of the single-degree-of-freedom oscillator with central circular frequency ω_0.

Using the standard random vibration method and the empirical formulas[12] for the mean peak value and its standard deviation of a stationary Gaussian process, the mean peak displacement response and its coefficients of variation can be calculated. By varying the natural frequency ω_0 in the calculation, the response spectrum is obtained.

Figure 4 shows the calculated mean response spectra and their corresponding coefficients of variation of the translational and torsional motions. They are calculated by using the parameters representing a typical medium firm soil site with $\omega_g = 2{\cdot}5$ Hz and $\xi_g = 0{\cdot}6$; the scale factor $\Gamma = 1000\ \text{cm}^2/\text{s}^3$, duration $T = 20$ s, and those constants corresponding to Event 45 as given in Table I for the coherency function. As can be seen,

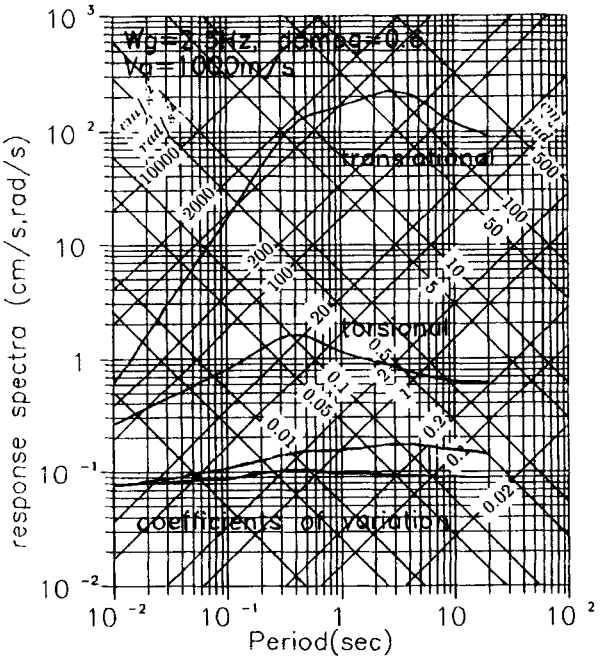

Figure 4. Velocity response spectra and their coefficients of variation of translational and torsional motions

the peak value of the torsional motion response spectrum occurs at $T = 0{\cdot}4$ s, or corresponds to the central frequency of the translational motion PSD. It is also relatively flatter as compared with the translational motion response spectrum. The translational motion response spectrum decreases rapidly at both small and large periods. This implies that the translational ground motion energy is more concentrated in a small period band while that of the torsional motion is more evenly distributed.

Compared to the mean response spectra, the coefficients of variation of both the translational and the torsional motion response spectra are small, implying that the estimated mean peak response values reflect the true characteristics of the response spectra.

The effects of the coherency function and the site conditions on the response spectra of the torsional motions with respect to the corresponding translational motions are discussed in the following.

Effect of coherency loss function

Three sets of constants are used to model the coherency loss function. They are: $a_j = 1{\cdot}0 \times 10^{-7}$, $b_j = 1{\cdot}16$ (coherency 1); $a_j = 5{\cdot}0 \times 10^{-6}$, $b_j = 2{\cdot}0$ (coherency 3), $j = 1, 2$; and those constants corresponding to Event 45 as given in Table I (coherency 2). These three sets of constants result in high (coherency 1), low (coherency 3) and medium (coherency 2) cross-correlations between the spatially varying ground motions. Figure 5 shows the coherency loss functions with separation distances $x = 188$ m and $y = 68$ m.

The torsional motion response spectra corresponding to the three coherency loss functions and the medium firm soil site with an apparent velocity $v_a = 1000$ m/s are shown in Figure 6. The response spectrum calculated by considering the phase shift only, i.e. $|\gamma_{kl}| = 1{\cdot}0$ or $\alpha_1(\bar{\omega}) = \alpha_2(\bar{\omega}) = 0{\cdot}0$ in equation (9), is also shown for comparison purpose. It can be seen that the coherency loss effect affects the torsional motion response spectrum substantially at large periods. The less correlated motions result in a higher torsional motion response spectrum. The coherency loss effect, however, is not pronounced at small period. This is because, at small periods or high frequencies, the values of the parameter functions $\alpha_j(\bar{\omega})$ in equation (9) are much smaller than that of $\bar{\omega}/2v_a^2$. Thus, the torsional ground motion is mainly caused by the phase shift effect (reflected by $\bar{\omega}/2v_a^2$), the coherency loss effect (reflected by $\alpha_j(\bar{\omega})$) is insignificant as compared to the phase shift effect. As the period increases, the coherency loss effect becomes pronounced since at large periods or low frequencies, the $\alpha_j(\bar{\omega})$ function values are comparable to or even greater than $\bar{\omega}/2v_a^2$.

The previous methods[2,3] of estimating the torsional ground motions only considered the phase shift of the propagating plane wave owing to lack of the ground motion coherency loss data. As can be seen, considering

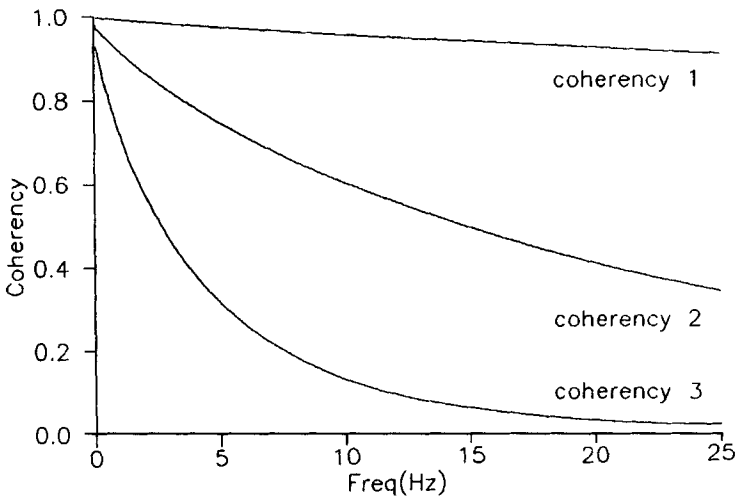

Figure 5. Three coherency loss functions

the phase shift only can well-predict the torsional motion response spectrum at small period, or when the spatially varying ground motions are highly correlated (coherency 1). When spatial ground motions are only weakly correlated, however, neglecting the coherency loss between the spatial ground motions underestimates the torsional motion response spectrum. The underestimation could be more than 30 per cent at large periods.

Figure 7 shows the velocity response spectrum ratios of the torsional to lateral ground motions and the corresponding normalized coefficients of variation of the torsional response spectra, where the coefficients of variation are also normalized by the translational velocity response spectrum. As can be seen, the velocity

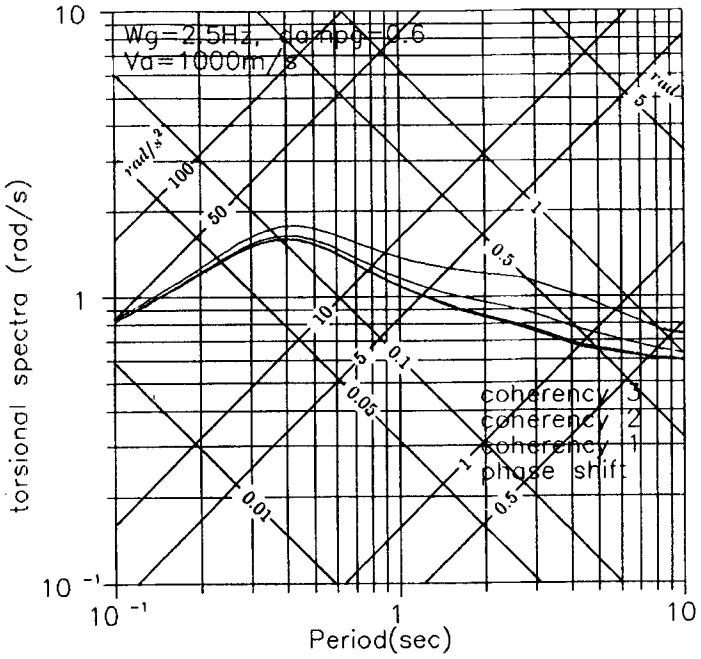

Figure 6. Torsional motion response spectra corresponding to different coherency functions

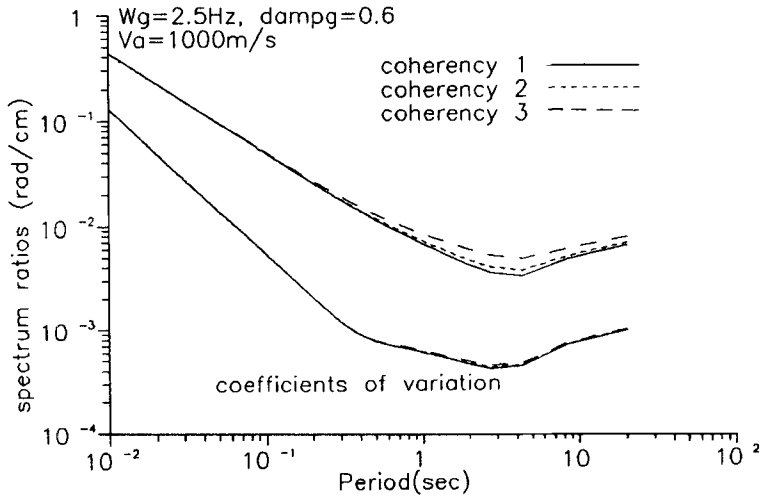

Figure 7. Velocity response spectrum ratios and their coefficients of variation

response spectrum ratios decrease almost log linearly in the period range from 0·01 s to about 4 s, and then increase from 4 to 25 s. This is because, as also shown in Figure 4, the torsional ground motion energy is more evenly distributed than that of the translational motions.

The minimum values of the response spectrum ratios occur at about 4 s or frequency 0·25 Hz. This corresponds to the central frequency of the high-pass filter $\omega_1 = 1{\cdot}636$ rad/s = 0·26 Hz. Figure 8 shows the response spectrum ratios and the corresponding normalized coefficients of variation obtained by using the same parameters except that the central frequency of the high-pass filter is changed to $\omega_1 = 1{\cdot}0$ Hz. As can be seen, the minimum values of the response spectrum ratios occur at a period about 1 s, and the corresponding minimum values are larger than those obtained with $\omega_1 = 1{\cdot}636$ rad/s. These observations indicate that the high-pass filter used in modelling the translational ground motions, which has little effect on the translational motion response spectrum and is just applied to attenuate the very low-frequency energy to correct the possible drifting in ground velocity and displacement,[11] affects the torsional ground motion response spectrum substantially.

Effect of apparent velocity

Figure 9 shows the response spectrum ratios and their normalized coefficients of variation obtained by using $\omega_g = 2{\cdot}5$ Hz, $\xi_g = 0{\cdot}6$, coherency loss function 2, and different apparent propagation velocities. As can be seen, the normalized coefficients of variation are almost independent of the apparent velocity, while the response spectrum ratios depend on it. The response spectrum ratios are larger if the ground motion apparent velocity is lower. This is because a low apparent velocity results in a large phase difference between the spatial translational motions. These results indicate that the effect of phase difference is very significant throughout the period range. As also can be noted the response spectrum ratios increase almost proportionally as the apparent velocity decreases. For example, at period 0·01 s, the response spectrum ratios are about 8, 4, and 2 for the apparent velocities of 500, 1000 and 2000 m/s, respectively.

The apparent velocity of a site is approximately determined if its average shear wave velocity and the ground motion incident angle are known. However, in many cases the incident angle is not known, then the average shear wave velocity of the site under consideration might be used to estimate the torsional ground motions. This approximation will lead to an over-estimation of the torsional ground motions as the average shear wave velocity is the lower limit of the apparent propagation velocity.

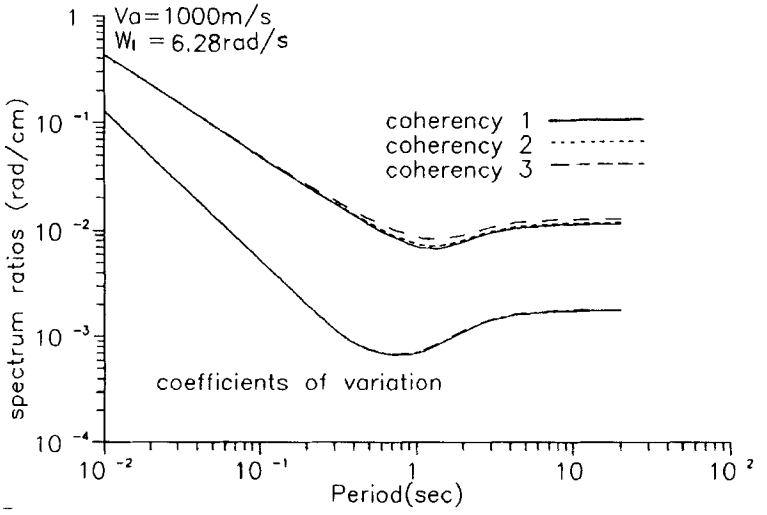

Figure 8. Velocity response spectrum ratios and their coefficients of variation obtained by using a different central frequency W_1

Effect of site conditions

The response spectrum ratios corresponding to the three site conditions are calculated. They are the firm site with $\omega_g = 5{\cdot}0$ Hz and $\xi_g = 0{\cdot}2$, the medium firm site with $\omega_g = 2{\cdot}5$ Hz and $\xi_g = 0{\cdot}6$ and the soft site with $\omega_g = 1{\cdot}0$ Hz and $\xi_g = 0{\cdot}8$. The apparent velocity $v_a = 1000$ m/s and the coherency loss function 2 are used in the calculation. The results are shown in Figure 10. As can be noted, the response spectrum ratios have the similar shape and are almost identical when the period is smaller than 0·2 s. This is because the phase shift effect is so dominating at small periods that the change of the site conditions has little effect on the response spectrum ratios. The site conditions affect the response spectrum ratios when period is larger than 0·2 s. The response spectrum ratios corresponding to the firm site are the largest while those corresponding to the soft site are the smallest. This is because the translational ground motion energy is more concentrated in a small period band centred at $1/\omega_g$. For example, at a large period, the translational motion response spectrum of a firm site with a small central period $1/\omega_g$ is smaller than that of a soft site with a large central period $1/\omega_g$

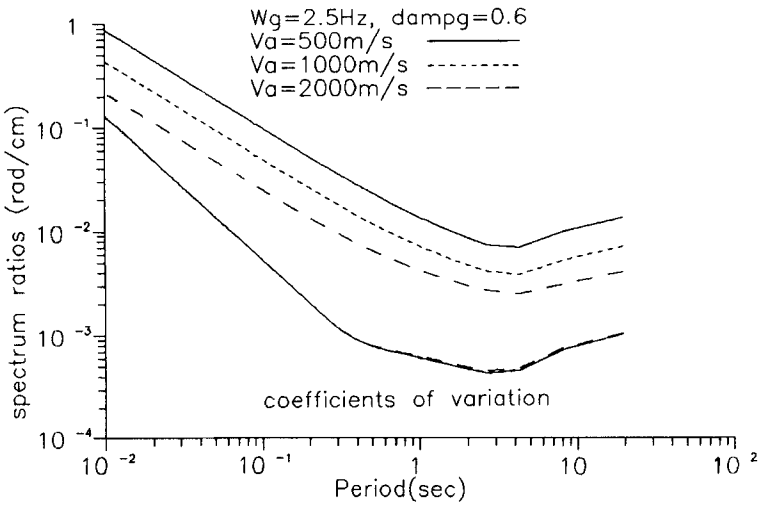

Figure 9. Response spectrum ratios and their coefficients of variation corresponding to the different apparent velocities

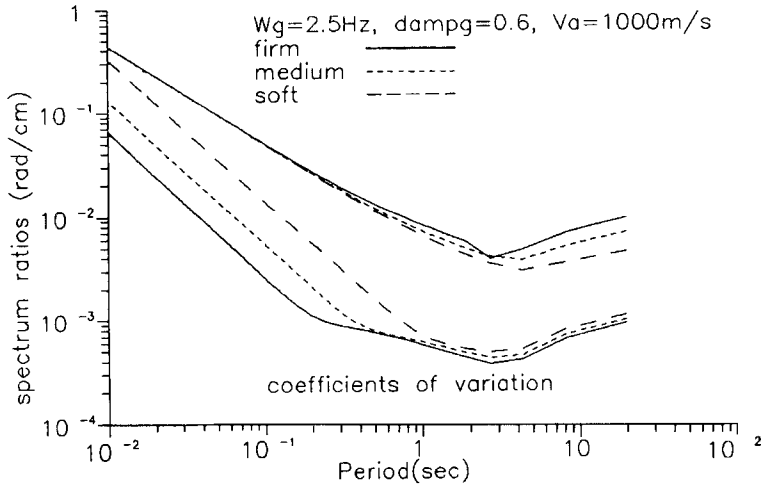

Figure 10. Response spectrum ratios and their coefficients of variation corresponding to the different site conditions

due to dynamic amplification effect, while the difference between the torsional motion response spectra of different sites is not as significant because the torsional motion energy is more evenly distributed over the periods. Thus, the response spectrum ratios of the firm site is larger than those of the soft site at large periods.

The corresponding normalized coefficients of variation strongly depend on the site conditions. The coefficients of variation of the firm site are the smallest and those of the soft site are the largest. At small period, the normalized coefficients of variation of the soft site are comparable to the response spectrum ratios. However, as the period increases, the normalized coefficients of variation of the three sites decrease and become small compared to the corresponding response spectrum ratios.

CONCLUSIONS

It was found that the exponential coherency loss function should be a function of the square of the seperation distance in order to calculate the torsional ground motion power spectral density. Thus, a new form of empirical coherency function has been suggested. It was obtained by analysing the recorded spatially varying ground motions at the SMART-1 array. The proposed coherency function has been verified to give reliable estimation of the coherency of the spatially varying translational ground motions.

The power spectral density function of torsional ground motion at a point on ground surface has been derived. It depends on the power spectral density function and the coherency function of the spatially varying translational ground motions. The torsional ground motion power spectral density function has also been tested to yield reliable estimation.

With the commonly used translational ground motion power spectral density function and the proposed coherency function, the random vibration method has been employed to estimate the torsional and translational motion response spectra. The effects of the coherency functions and the site conditions on the torsional motion response spectrum have been discussed. The ratios of the torsional to translational ground motion response spectra have been presented and discussed. These ratios can be used to estimate the torsional motion response spectra based on the known translational motion response spectra.

ACKNOWLEDGEMENT

The SMART-1 data used in this study were provided by Dr. Bruce A. Bolt, professor emeritus, Department of Geology and Geophysics, University of California at Berkeley, whose constant encouragement and help are greatly acknowledged.

REFERENCES

1. B. A. Bolt, C. H. Loh, J. Penzien, Y. B. Tsai and Y. T. Yeh, 'Preliminary report on the SMART-1 strong motion array in Taiwan', *Report No. UCB/EERC-82-13*, Earthquake Eng. Research Center, Univ. of California at Berkeley, CA, 1982.
2. N. M. Newmark, 'Torsion in symmetrical buildings', *Proc. 4WCEE*, Santiago, Chile, Vol. 2, a3/19–a3/32, 1969.
3. W. K. Tso and T. I. Hsu, 'Torsional spectrum for earthquake motions', *Earthquake eng. struct. dyn.* **6**, 375–382 (1978).
4. C. S. Oliveira and B. A. Bolt, 'Rotational components of surface strong ground motions', *Earthquake eng. struct. dyn.* **18**, 517–528 (1989).
5. J. C. De La Llera and A. K. Chopra, 'Evaluation of code accidental-torsion provisions from building records', *J. struct. eng. ASCE* **120**, 597–616 (1994).
6. N. A. Abrahamson, 'Estimation of seismic wave coherency and rupture velocity using SMART-1 strong-motion array recordings', *Report No. UCB/EERC-85-02*, Earthquake Eng. Research Center, University of California at Berkeley, CA, 1985.
7. R. S. Harichandran and E. H. Vanmarcke, 'Stochastic variation of earthquake ground motion in space and time', *J. eng. mech. ASCE*, **112**, 154–174 (1986).
8. C. H. Loh and Y. T. Yeh, 'Spatial variation and stochastic modelling of seismic differential ground movement', *Earthquake eng. struct. dyn.* **15**, 583–596 (1988).
9. H. Hao, C. S. Oliveira and J. Penzien, 'Multiple-station ground motion processing and simulation based on SMART-1 array data', *Nuclear eng. des.* **111**, 293–310 (1989).
10. J. Penzien and M. Watabe, 'Characteristics of 3-dimensional earthquake ground motions', *Earthquake eng. struct. dyn.* **3**, 365–373 (1975).
11. R. Ruiz and J. Penzien, 'Probabilistic study of the behaviour of structures during earthquakes', *Report No. UCB/EERC 69-03*, Earthquake Eng. Research Center, University of California at Berkeley, CA, 1969.
12. A. Der Kiureghian, 'Structural response to stationary excitation', *J. eng. mech. div. ASCE*, **106**, 1195–1213 (1980).